Bioresource Technology 159 (2014) 215–222

Contents lists available at ScienceDirect

Bioresource Technology

journal homepage: www.elsevier.com/locate/biortech

An experimental and theoretical investigation on torrefaction of a large wet wood particle

Prabir Basu[a], Anup Kumar Sadhukhan[b,*], Parthapratim Gupta[b], Shailendra Rao[c], Alok Dhungana[c], Bishnu Acharya[c]

[a] Mechanical Engineering Department, Dalhousie University Halifax, Canada
[b] Chemical Engineering Department, National Institute of Technology Durgapur, India
[c] Greenfield Research Incorporated, Halifax, Canada

HIGHLIGHTS

- A simple kinetic model proposed for primary and secondary torrefaction reactions.
- Drying and 1D heat transfer model incorporated.
- Torrefaction reaction identified as exothermic for Popler wood.
- Optimum torrefaction temperature, particle size and residence time determined.

GRAPHICAL ABSTRACT

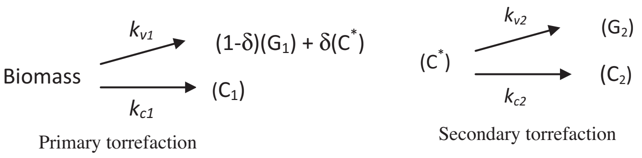

ARTICLE INFO

Article history:
Received 13 December 2013
Received in revised form 14 February 2014
Accepted 17 February 2014
Available online 4 March 2014

Keywords:
Torrefaction
Kinetic model
Heat transfer
Rate-controlling
Design

ABSTRACT

A competitive kinetic scheme representing primary and secondary reactions is proposed for torrefaction of large wet wood particles. Drying and diffusive, convective and radiative mode of heat transfer is considered including particle shrinking during torrefaction. The model prediction compares well with the experimental results of both mass fraction residue and temperature profiles for biomass particles. The effect of temperature, residence time and particle size on torrefaction of cylindrical wood particles is investigated through model simulations. For large biomass particles heat transfer is identified as one of the controlling factor for torrefaction. The optimum torrefaction temperature, residence time and particle size are identified. The model may thus be integrated with CFD analysis to estimate the performance of an existing torrefier for a given feedstock. The performance analysis may also provide useful insight for design and development of an efficient torrefier.

© 2014 Elsevier Ltd. All rights reserved.

1. Introduction

The independence and self-sufficiency in energy sector is an indicator of the socio- economic development of any country. Hence the recent research trend focuses towards the exploration of energy by utilization of non-conventional energy sources. A major thrust is on efficient and regulated utilization of the abundantly available natural and renewable resource, the biomass. Biomass provides a clean, renewable energy source the use of which could significantly improve our environment, economy and energy security by reducing the consumption of fossil fuels, emission of greenhouse gasses and environmental pollution (Chen and Kuo, 2011). Biomass can be used to generate heat and power as per the requirement of industry and domestic uses. This unique advantage over wind power and solar energy via photovoltaic cells makes biomass an important pillar in the energy supply today and in the foreseeable future. Biomass, including a wide range of fuels such as wood, energy crops, forest and agricultural residue, industrial and municipal wastes etc., may be the promising

---

[*] Corresponding author. Tel.: +91 9775390738; fax: +91 343 2754078.
E-mail address: t_sadhu@yahoo.com (A.K. Sadhukhan).

http://dx.doi.org/10.1016/j.biortech.2014.02.105
0960-8524/© 2014 Elsevier Ltd. All rights reserved.

alternatives for coal. Biomass is predominantly used in unscientific manner in rural areas for cooking and heating purposes. However, the utilization of biomass in an industrial scale is a real challenge. The inherent properties of biomass like high moisture content, low energy density and difficulty in grinding limit its use in coal-fired power plants for co-firing option. Furthermore, the biological decay of biomass during storage possesses additional risk of fire and safety issue during storage. To overcome these limitations, torrefaction has been proposed as a process for upgrading biomass by thermal treatment (Arias et al., 2008).

Torrefaction is a kind of mild pyrolysis in temperatures ranging from 200 to 300 °C and the residence time varies from about an hour to several hours in the absence of oxygen (Li et al., 2012). Ciolkosz and Wallace (2011) presented an overview of the influence of torrefaction temperature and residence time on important fuel parameters like chemical composition, heating value and grindability. The researchers also investigated the heat of reaction by monitoring the energy demand of the torrefaction reactor as the heat of reaction is an important parameter for the control of large-scale torrefaction plants.

During the Torrefaction process, mostly the hemicellulose in biomass depolymerizes releasing volatiles of low energy values and, as a result, the remaining solid has high energy density. This process effectively reduces the H/C and O/C ratio in biomass (Sarvaramini et al., 2013), bringing it closer to coal in terms of combustion properties. Moreover, substantial changes in physical properties like increase in grindability, hydrophobicity (Li et al., 2012) also takes place, making it easier to handle and process as a fuel.

Torrefaction is currently being considered as one of the most suitable pre-treatment process for biomass feedstock, particularly for thermal conversion like pyrolysis, combustion, gasification and co-firing system. Torrefaction not only improves the grindability and energy density, it also improves uniformity in properties among different biomass feedstock types and eliminates volatile acids content in bio-oil extracted from a mixture of biomass feed stock. It also improves fluidisation properties of heterogeneous biomass mixture of varying sources (Kersten et al., 2005). There is an enormous potential for utilization of torrefied biomass for co-firing in existing coal fired power plants. With the rise in interest in co-firing, the need for a first-level model for torrefaction process is more pronounced than before. For the design of a new torrefier for a specific type of feed as well as torrefaction of a new feedstock in an existing torrefier, it is vital to know the product quality for a given torrefaction temperature, and residence time. Although pilot plant tests are the best option, it is expensive and may not allow exploration of all variables, while a suitable mathematical model is expected to provide the vital information about the process.

Torrefaction of fine particles of biomass may be considered to be kinetically controlled where transfer resistances can be neglected. Typically, the most simplified kinetic model for torrefaction reaction may be represented by the following equation (Sadhukhan et al., 2008; Murugan et al., 2009).

$$\frac{dX}{dt} = k.(1-X)^n \tag{1}$$

Where X is the fractional conversion on dry ash free basis and is defined as:

$$X = \frac{w_i - w}{w_i - w_{\text{ash}}} \tag{2}$$

w is the mass of the biomass sample at time t, w_i is the initial mass of the sample and w_{ash} is the mass of ash in the sample calculated from proximate analysis, all considered on dry basis. k is the reaction rate constant that usually follows the Arrhenius dependence on temperature. Di Blasi (2008) proposed that the pyrolysis of biomass at low temperature may be presented by a global one step reaction kinetics for overall decomposition but the kinetic parameters obtained by different researchers are not consistent with this model.

The micro fibrous wood has a complex structure made of three main constituents; cellulose, hemicelluloses and lignin (Chen and Kuo, 2011). They proposed that the torrefaction kinetics of wood might be represented by the individual degradation kinetics of cellulose, hemicelluloses and lignin with three n^{th} order chemical reactions. Torrefaction of wood based on thermal degradation kinetics of hemicellulose, cellulose and lignin lead to several thermal events detected by sudden changes in slope of mass loss vs. temperature curves (Sadhukhan et al., 2008).

As torrefaction of wood may be considered to be pyrolysis at low temperature, pyrolysis models are expected to be applicable for torrefaction of biomass without major error. The kinetic model by Bradbury et al. (1979) consisting of an activation step followed by two subsequent reactions may be used. Varhegyei et al. (2011) proposed another model consisting of two first-order consecutive reactions incorporating decomposition of Xylan. They assumed that xylan produces an intermediate product, which reacts further to produce the final product.

Another model was developed by Rousset et al. (2006) incorporating the constituent's lignin, cellulose, and hemicelluloses in proportion with their mass fraction in wood. It was assumed that lignin decomposes into char and volatiles in a simple decomposition path. Cellulose decomposes by two competing reactions, one producing tar and the other producing char and volatiles. Hemicellulose decomposes according to parallel reaction scheme to produce char and volatiles with the creation of an intermediate product. The model involves a large number of kinetic parameters. Di Blasi and Lanzetta (1997) modelled the torrefaction kinetics by a two-step reaction mechanism with competing reactions for the formation of solid char and volatiles. Prins et al. (2006) used this reaction scheme for torrefaction kinetics of beech and willow wood fines in isothermal TGA apparatus. They estimated the kinetic parameters and found that the activation energies for formation of gaseous volatiles are higher than that of formation of chars, which ensures that the volatile yield increases compared to char with an increase in reaction temperature. Sadhukhan et al. (2009) also observed experimentally a similar trend for pyrolysis of wood.

Biomass being fibrous in nature has poor grindability. The preparation of biomass fines is not only an energy-intensive process but also need the special design for milling system. As torrefaction significantly improves the grindability of biomass (Arias et al., 2008), large biomass particles are better suited. The torrefaction of thick wood particles involves a strong interaction between reaction kinetics and heat transfer phenomena at the level of both single particles and the reaction environment. When exposed in a high-temperature environment, the particle is initially heated up by external convection and radiation depending on the temperature. Transient heat conduction and internal convection take place within the particle, followed by highly endothermic moisture evaporation depending on the initial moisture content. Meanwhile, the already dried region of the particle near the outer surface undergoes thermal degradation. Therefore, the different spatial zones may appear during the process of transient torrefaction; a char layer, a torrefaction region, a drying region and the virgin moist biomass. Water vapour and gaseous volatiles partly leave the particle flowing through the porous structure of solid biomass. The volatiles produced at inner depth of thick biomass particle passes through the pores very slowly. A fraction of volatiles may be deposited on char surface (Koufopanos et al., 1991) and may undergo secondary reactions over char surface at high temperature. These are either cracking reactions to give light hydrocarbon or re-polymerization to produce secondary char (Di blasi, 1996).

Chen et al. (2014), based on isothermal and non-isothermal torrefaction kinetics of microalgae in TGA, proposed a four-stage decomposition depending on the torrefaction temperature. They reported that for the same reactor temperature and residence time, heating rate and heating control (non-isothermal or isothermal) greatly affects the yield of final residue.

Bates and Ghoniem (2013) proposed that the first stage of torrefaction, associated with hemicellulose decomposition, is exothermic in nature releasing 40–280 kJ/kg of willow wood. The second stage is associated with the decomposition of the remaining lignocellulosic components, completes after a longer period, and is predicted to be either endothermic or exothermic depending on the temperature, compositions and solid properties. Both the rate of mass loss and rate of heat release increase at higher temperatures.

Microwave torrefaction of rice straw and pennisetum (Huang et al., 2012) at various heating rate and final temperatures reveals that the activation energy lies between 11 and 14 kJ/mol which is different from the thermal decomposition of pure hemicellulose, cellulose or lignin. They proposed that the variation is due to the factors such as heating manner, heating rate, and reaction mechanism.

Experimental results by Chen et al. (2013) suggested that the torrefaction reaction of biomass materials (palm fibre, coconut fibre, eucalyptus, and *cryptomeria japonica*) is controlled by chemical kinetics and physical processes like heat and mass transfer within the biomass and the solid yield of biomass is not affected by the superficial velocity of N_2 at a given temperature.

In the present work, the kinetic model for large cylindrical poplar wood particles considers primary reactions with deposition coefficient for primary gaseous volatiles along with secondary reactions. The kinetic model is coupled with heat transfer that includes conductive, convective and radiative modes of heat transfer. The shrinkage in particle is also considered. For fine wood particles, only the primary reaction is considered without any deposition. The model is first validated and then used to carry out simulation studies. Optimum particle size and reactor temperature are determined for torrefaction of large size wood particles. Such simple models are often suited for integration into the CFD code for development of efficient reactor in industrial practise. The present work is a product of scientific collaboration between the National Institute of Technology Durgapur, India, Dalhousie University, Canada and Greenfield Research Incorporated of Halifax, Canada.

2. Methods

2.1. Biomass sample

Fine saw dust (100–500 micron) collected from sawing poplar dowels is used as the fine biomass sample for this study. Proximate and ultimate analyses of the sample are shown in Table 1. Cylindrical poplar dowels, 152.4 mm long and 25.4 mm in diameter are used as large biomass particle samples. The L/D ratio of 6 is high enough to consider one-dimensional model so that the heat transfer in axial direction may be neglected.

Table 1
Properties of Poplar wood fines (wb–wet basis; db–dry basis; daf–dry ash free basis).

Biomass size range 100–500 micron			
Proximate analysis		Ultimate analysis	
Moisture (wb)	6.4%	Carbon (daf)	51.25%
Volatiles (db)	78.68%	Hydrogen (daf)	7.92%
Fixed carbon (db)	19.58%	Nitrogen (daf)	0.06%
Ash (db)	1.84%	Sulphur (daf)	3.02%
		Oxygen (daf)	35.62%

2.2. Experimental

The experimental setup consists of a custom-designed thermogravimetric unit. It has a 42 mm diameter and 1.2 m long stainless steel tube as a reactor, heated by a set of 2.4 kW annular electric heaters surrounding it with a capacity to heat it up to 900 °C. Biomass sample is packed in a quartz wool matrix typically in a lump of 0.25 gm. It is kept in a perforated basket, which is suspended from the mass balance inside the reactor (Fig. 1). The mass balance with least count of 0.1 mg records the mass of the biomass continuously to the computer.

The unit is continuously flushed by Nitrogen at 3 litres per minute (lpm). Before the gas is released at the bottom of the reactor, it is preheated through a tube coiling around the outside surface of the reactor. The temperature of the reactor zone is measured by a thermocouple, whose data is also logged in a computer.

Before starting the experiment, the reactor is preheated to the desired temperature for 30 min. Then the basket filled with the saw dust is lowered into the reactor and suspended from the bottom of the mass balance. The data logger in the computer measures both mass and the temperature. The reaction time (or residence time) is recorded once the biomass is loaded in the reactor. The mass loss data of the biomass stored in the computer is plotted and fed as an input to the model. Similarly the wood cylinder is wrapped around by fine nichrome wires, acting as a cage, and is tied to a wire hanging from the balance. The sample is introduced into the reactor in presence of nitrogen gas flow. The mass-loss is monitored continuously at reactor temperature of 200–300 °C.

A fine hole is drilled up to the centre in the wood cylinder and a fine sheathed Chromel–Alumel thermocouple is inserted to measure the centre point temperature. Another thermocouple is fixed at a radial distance of $r_s/2$. Both the thermocouples are plugged by iron-cement so as to ensure uniform reaction conditions.

2.3. Models

The chemical composition of biomass is heterogeneous in nature and the products from torrefaction are even more heterogeneous. Hence, modelling of torrefaction is always associated with a large degree of approximation, assumptions and lumping of components to reduce the number of model parameters and ensure manageability of the model equations. This simple model, as

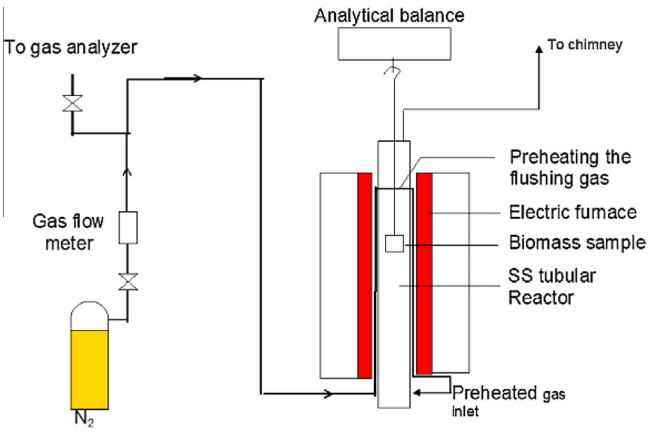

Fig. 1. Schematic diagram of the experimental set-up.

mechanistic as possible and with minimum number of parameters, would be ideal for design and analysis of reactors. Of course, it should be able to predict the performance of a torrefier over a given range of operating parameters. Even without denying the needs for more involved models involving the product composition and intra-particle details, such simple models are often better suited for integration into CFD code for development of efficient reactor for industrial practise. Keeping that in mind, the present work primarily focuses on developing a simple but reasonably accurate model for explaining the torrefaction behaviour both for biomass fines and large wet cylindrical particles. The proposed model includes drying, heat transfer resistances and shrinkage during torrefaction of wet wood cylinder.

2.3.1. Drying model

In the present study a simplified model (Saastamoinen et al., 2000) is used for drying of wood cylinders with a first order rate equation and Arrhenius-type temperature-dependence.

$$(-r_d) = \rho_s \frac{dX}{dt} = k_d e^{-E_d/\mathrm{RT}}.X \tag{3}$$

r_d is the drying rate, ρ_s is density of solid and X is kg of moisture in the sample per kg of dry sample. The rate parameters (k_d, E_d) for drying operations are taken after Saastamoinen et al. (2000). The temperature of the particle during drying is estimated by the energy balance equation presented later in this section (Eq. (14)).

2.3.2. Kinetic model for torrefaction of wood

The proposed kinetic model incorporates primary and secondary reactions. The primary reaction model consists of two parallel reactions resulting in primary volatiles and primary char, C_1. For large biomass particles, a fraction of the primary volatiles and gases, rich in heavier hydrocarbon and having lower permeability, gets deposited on hot primary char surface with deposition coefficient, δ, and is denoted by C^*. The rest of the primary gases, G_1, rich in lighter hydrocarbons, are released through the pore matrix. For wood fines, however, the primary volatiles leave the particle before deposition and δ may be considered to be 0.

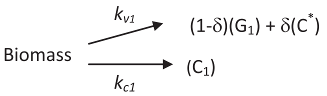

(4)

However during torrefaction of large size wood particles a part of the primary volatiles gets deposited on char surface as C^* and undergoes secondary reaction on hot char surface. The secondary reaction rate is highly influenced by the residence time and heat transfer rate. The secondary reaction includes two competitive reactions; (i) cracking reaction to produce light hydrocarbons called secondary gases, G_2 and (ii) re-polymerization reaction to produce secondary char, C_2.

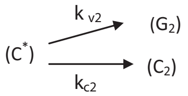

(5)

The secondary reaction is assumed to occur within the pores of solid matrix and the rate is proportional to the concentration of the C^* (Boroson et al., 1989).The model equations are:

$$\frac{dB}{dt} = -(k_{v1} + k_{c1}).B^n \tag{6}$$

$$\frac{dC^*}{dt} = \delta k_{v1}.B^n - (k_{v2} + k_{c2}).C^* \tag{7}$$

$$\frac{dC_1}{dt} = k_{c1}.B^n \tag{8}$$

$$\frac{dC_2}{dt} = k_{c2}.C^* \tag{9}$$

The residual mass fraction W at any time instant is written as:

$$W = B + C_1 + C^* + C_2 \tag{10}$$

$$\text{At } t = 0, B = 1, C_1 = 0, C_2 = 0, C^* = 0 \tag{11}$$

Changes in the volume of the reacting solid are experimentally investigated by the present authors. The variation of density for shrinking biomass particle during torrefaction may be written as:

$$\frac{\partial \rho_s}{\partial t} = \rho_{s0}\frac{\partial W}{\partial t} - \frac{\rho_s}{\Omega}\frac{\partial \Omega}{\partial t} \tag{12}$$

The instantaneous volume of the reacting biomass particle, Ω, is assumed to vary as:

$$\Omega = \Omega_0.f_r^{v+1} \tag{13}$$

The value of v is 1 for cylindrical biomass particle. Shrinkage factor f_r in radial direction only is considered in the present 1-D model and is estimated from experimentally measured dimensions of the residual char after torrefaction, assuming that the geometric structure integrity is retained with no fragmentation. L/D ratio of 6 used in the work is high enough for applicability of 1-D model (Kersten et al., 2005). The instantaneous shrinkage factor is estimated by linear interpolation using final shrinkage values and degree of conversion after Bryden and Hagge (2003). The experimentally obtained final shrinkage in radial direction was observed to be 9% at 200 °C and 20% at 300 °C.

2.3.3. Heat transfer model

Considering the heat of reactions of moisture evaporation and torrefaction for a shrinking biomass particle the energy conservation equation may be given as:

$$\frac{\partial}{\partial t}(\rho_s\ c_{ps}T) = \frac{1}{r^v}\frac{\partial}{\partial r}(\lambda_e r^v \frac{\partial T}{\partial r}) + (-\Delta H)(-\frac{\partial \rho_s}{\partial t}) + (-\Delta H_d) \times (-r_d) - \frac{(\rho_s\ c_{ps}T)}{\Omega}\frac{\partial \Omega}{\partial t} \tag{14}$$

The initial and boundary conditions are:

$$\text{at } t = 0, \text{and } 0 \leqslant r \leqslant r_s, T = T^0 \tag{15}$$

$$\text{for } t > 0, \text{at } r = 0, \frac{\partial T}{\partial r} = 0(\text{due to symmetry}) \tag{16}$$

$$\text{for } t > 0, \text{at } r = r_s, -\lambda_e\frac{\partial T}{\partial r} = h_c(T - T_f) + \varepsilon\sigma(T^4 - T_f^4) \tag{17}$$

2.3.4. Numerical solution

The governing differential Eqs. (6), (7), (8), (9), and (12) along with the initial condition (Eq. (11)) are solved simultaneously to determine the primary variables B, C_1, C_2, and C^* at any radial position in the cylindrical wood particle at different time instants. Eqs. (6), (7), (8), (9), and (12) are solved at a particular radial position using fourth order Runge–Kutta–Gill method with a fixed time step size. The governing energy equation (Eq. (14)) and the initial and boundary conditions (Eqs. (15)–(17)) poses a moving boundary problem due to continuous size change. Transformation of space coordinate is generally employed to solve such moving boundary problems. However, in this work the dimensional differential equation along with the initial and boundary conditions are solved simultaneously to determine the temperature T as functions of time and radial position. Similar technique was adopted by Di Blasi (1996) to solve such moving boundary problems. Implicit finite volume method based on central differencing scheme (Patankar,

1980) is employed for solving the energy equation. A FORTRAN code is developed to solve all the mass and energy governing equations simultaneously.

3. Results and discussion

3.1. Torrefaction of wood fines

3.1.2. Experimental results

The experimentally measured historical profiles of residual mass of dry poplar wood at given temperatures are converted to residual mass fraction on dry ash-free basis (Fig. 2) during torrefaction at six different temperatures in the range 200–300 °C. Mass loss is observed at a temperature as low as 200 °C, though it is very slow; only 1.2% after 15 min. Thermal degradation of biomass starts with xylan at a temperature of 182 °C (Chen and Kuo, 2011) with a very slow rate and only about 10% mass loss is observed after a time of 150 min at 200 °C. As the temperature rises, the mass-loss rate gradually increases reducing the mass yield of torrefaction. The thermal degradation of cellulose does not start below 250 °C (Gaur and Reed, 1998). Hence, the mass loss curve at 260 °C lies far apart from that at 240 °C indicating start of cellulose decomposition. At 300 °C the rate of degradation becomes much faster and the final yield is reached within a short time of about 18 min.

3.1.3. Estimation of kinetic parameters for primary reactions

The experimental residual mass fraction data from torrefaction of dry poplar wood fines (Fig. 2) is fitted to the two-step kinetic model (Eq. (4)) using the Eqs. (6) and (8) with $\delta = 0$. The best-fit values of the kinetic parameters k_{c1} and k_{v1} are determined at each torrefaction temperature by fitting the experimental residual mass fraction data of wood fines to the model using Levenberg–Marquardt method (Sadhukhan, 2010) which minimises the objective function:

$$f(k_{v1}, k_{c1}) = \sum_{j=1}^{m} (w_{j,\mathrm{model}} - w_{j,\mathrm{expt}})^2 \tag{18}$$

On computation, the orders of all the reactions are found to be nearly unity and hence the reactions are considered to be of first order. The frequency factor and activation energy of primary torrefaction reactions are obtained from the slope and intercepts of the straight line plots of $\ln(k_i)$ vs. $1/T$ at 200, 240, 260 and 300 °C (Table 2).

3.1.3. Validation of the kinetic model for wood fines

The experimental data at 220 and 280 °C is used to validate the kinetic parameters which are obtained from other four sets of experimental data at 200, 240, 260 and 300 °C. It may be noted that the experimental data at 220 and 280 °C is not used for estimation of kinetic parameters. The model predictions at 220 and 280 °C are compared with the experimental TG data and the reaction rate profile (dry ash-free basis) (Fig. 3). The agreement is good in both cases with the mean relative errors being 0.056, 0.051 for fractional residue and 0.061 and 0.065 for reaction rate at 220 and 280 °C respectively. It is also observed from Fig. 3 that the reaction rate is uniformly low at 220 °C throughout the reaction period. At 280 °C the reaction rate is very high initially, decreasing rapidly with time. Further validation of the model is carried out with residual mass fraction after a reaction time of 9600 s (Table 3). A good agreement is observed between the model predictions and the experimental.

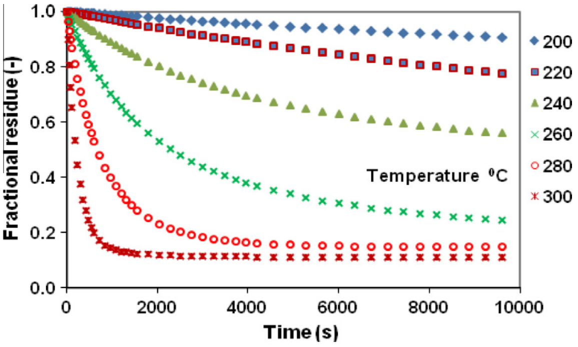

Fig. 2. Experimental residual mass fraction (daf basis) profiles at various temperatures for wood fines.

Table 2
Kinetic parameters of primary reaction for wood fines (100–500 micron).

	k_{v1}	k_{c1}
k^0 (s^{-1})	1.45E + 12	6.58E + 06
E (kJ/mol)	156.0	106.4

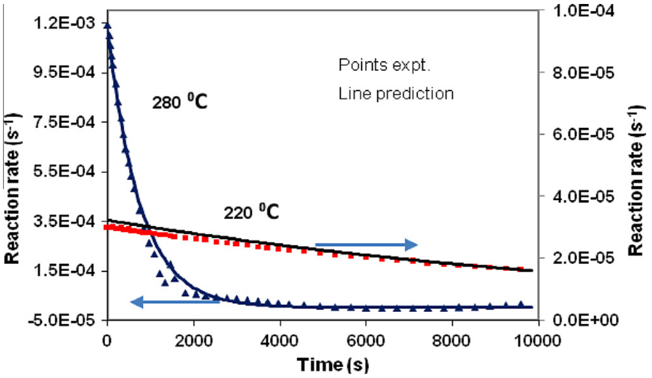

Fig. 3. Comparison of experimental reaction rate (daf basis) with model prediction for wood fines (points-experimental; lines-model prediction).

Table 3
Residual mass fraction after a reaction time of 9600 s for wood fines (100–500 micron).

Temp. (°C)	Expt. residue	Predicted residue	Difference
200	0.9059	0.9121	0.0062
220	0.7767	0.7711	0.0056
240	0.5588	0.5318	0.0270
260	0.2453	0.2386	0.0067
280	0.1493	0.1428	0.0065
300	0.1121	0.1109	0.0012

3.2. Torrefaction of large wet wood cylinder

3.2.1. Estimation of kinetic parameters for secondary reactions and heat of reaction

The deposition coefficient δ, the frequency factor and activation energy of secondary reactions are estimated by fitting the experimental mass-loss data of the wood cylinder to the model, while heat of reaction is estimated by fitting the experimental temperature profiles at the centre and at $r = r_s/2$ in the wood cylinder using Levenberg–Marquardt non-linear optimisation technique. The best-fit values of the parameters are presented in Table 4.

The activation energy for primary torrefaction reaction of wood fines (100–500 μm) is estimated to be 156.0 and 106.4 kJ/mol for volatiles and char formation respectively. The higher activation

Table 4
Kinetic parameters of secondary reactions for wood cylinder ($D = 25.4$ mm, $L = 152.4$ mm).

δ	k_{v2}	k_{c2}	(ΔH)
0.75	$k_{v20} = 6.17 \times 10^{12}\ \mathrm{s}^{-1}$ $E_3 = 184.1$ kJ/mol	$k_{c20} = 4.69 \times 10^{12}\ \mathrm{s}^{-1}$ $E_4 = 184.1$ kJ/mol	−360.1 kJ/kg

energy of volatile formation indicates that volatile formation reaction is more susceptible to temperature change than the char formation reaction. The pre-exponential factor for volatile formation is much higher than that for char formation (1.45×10^{12} and $6.58 \times 10^{6}\ \mathrm{s}^{-1}$ respectively). The values of kinetic parameters k_{v1} and k_{c1} are $8.58 \times 10^{-6}\ \mathrm{s}^{-1}$ and $1.17 \times 10^{-5}\ \mathrm{s}^{-1}$ respectively at 200 °C indicating that char formation rate is 1.36 times of that of volatile formation. However, at 300 °C the rate constants are $1.31 \times 10^{-3}\ \mathrm{s}^{-1}$ and $8.71 \times 10^{-3}\ \mathrm{s}^{-1}$ respectively, i.e. volatile formation rate is 6.66 times the char formation rate. Hence, though at low temperatures the char formation rate is more than that of volatile formation rate, the latter overtakes the former with an increase in temperature. Incidentally, secondary reactions do not take place for biomass fines.

For torrefaction of large wood particles (wood cylinders, 152.4 mm long and 25.4 mm in diameter), a part of the primary volatiles gets deposited on char surface as C^* and undergoes secondary reaction on hot char surface. The secondary reaction rate is highly influenced by the residence time and heat transfer rate. The intrinsic kinetic parameters for primary torrefaction reaction of wood cylinder are the same as that of wood fines. The activation energies for secondary torrefaction reactions of wood cylinder for volatiles and char formation are estimated to be 184.1 kJ/mol. This makes the secondary reaction more dominant at high temperature. Higher pre-exponential factor for secondary volatile formation than that of secondary char formation indicate that the mass loss during secondary reaction is more due to loss of secondary volatiles.

Prins et al. (2006) reported from TG mass loss experiments that the activation energy for primary torrefaction reactions of willow wood fines lies in the range 75–114 kJ/mol with pre-exponential factors between 2.48×10^{4} and $3.230 \times 10^{7}\ \mathrm{s}^{-1}$, while for the secondary reaction the activation energy and the pre-exponential factor are 151.7 kJ/mol and $1.1 \times 10^{10}\ \mathrm{s}^{-1}$ respectively. Rousset et al. (2006) proposed a network of 7 chemical reactions for primary and secondary decomposition of wood through an intermediate. The activation energy lies between 52.6 and 217.6 kJ/mol while the pre-exponential factors lie between 58.7 and $6.66 \times 10^{15}\ \mathrm{s}^{-1}$.

In the present study, the activation energy for primary torrefaction reaction is estimated to be 156 and 106.4 kJ/mol for volatiles and char formation while the pre-exponential factors are found to be 1.45×10^{12} and $6.58 \times 10^{6}\ \mathrm{s}^{-1}$ respectively (Table 2). The activation energy for the secondary torrefaction reaction for both volatiles and char formation are 184.1 kJ/mol with pre-exponential factors 6.17×10^{12} and $4.69 \times 10^{12}\ \mathrm{s}^{-1}$ respectively (Table 4).

The present study predicts higher activation energy for secondary reaction than Prins et al. (2006) perhaps due to complex network structure of intermediate C^* produced within the porous matrix of Poplar wood cylinder.

Bates and Ghoniem (2013) reported a heat of reaction of 40–280 kJ/kg for willow wood while in the present study it is found to be −360.1 kJ/kg for poplar wood.

3.2.2. Model validation for torrefaction of large wet wood cylinder

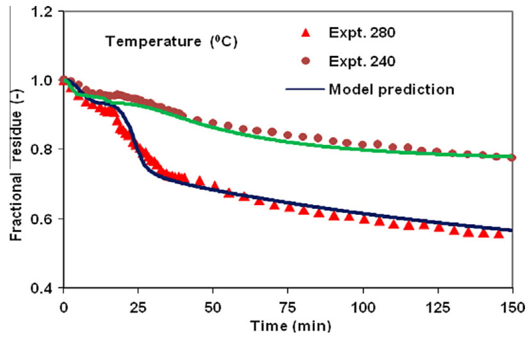

Fig. 4. Comparison of experimental fractional residue (ash-free basis) with model prediction ($D = 25.4$ mm, $L = 152.4$ mm).

Mass loss, centre and surface temperature profiles are obtained experimentally for wood cylinders at 200, 220, 240, 260, 280 and 300 °C. Of these six set of experiments, the data sets at 200, 220, 260 and 300 °C are employed to estimate the kinetic parameters, while the remaining two at 240 and 280 °C are used to validate the model (Fig. 4). The relative mean error between experimentally obtained mass residue and that predicted by the model are calculated for all data points at 240 and 280 °C are 0.041 and 0.039 respectively. The comparison of experimental centre temperature profiles with the model prediction is presented in Fig. 5. The relative mean error between experimentally obtained centre temperature and that predicted by the model for all data points at 240 and 280 °C are 0.044 and 0.047 respectively.

The experimentally obtained temperature profiles at the centre ($r = 0$) and mid-point ($r = r_s/2$) show that both temperatures are identical initially. But the particle surface gets heated up faster with time due to convective and radiative heat transfer and the mid-point temperature is slightly higher than the centre temperature due to less conductive resistance. However, when exothermic torrefaction reaction starts, heat is generated within the particle and the centre loses heat at a lower rate than the mid-point. As a result, both the temperatures become almost identical. The model predicts the same well.

3.3. Simulation studies for large wood particles

Torrefaction characteristics of large biomass particles are influenced by both chemical kinetics and heat transfer, which in turn depends on temperature, residence time and particle size. The final fractional residue reflects the degree of progress of reaction. Hence the effect of residence time on the final residual mass fraction is further assesed through model simulation for various particle diameter (with constant L of 152.4 mm).

3.3.1. Effect of temperature and residence time on torrefaction

The predicted effect of temperature and residence time on residual mass fraction is investigated for the wood cylinder of a

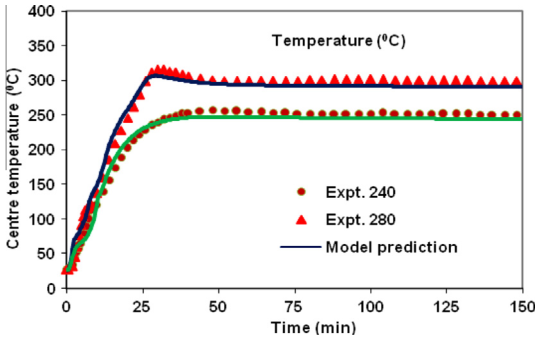

Fig. 5. Comparison of experimental centre temperature with model prediction ($D = 25.4$ mm, $L = 152.4$ mm).

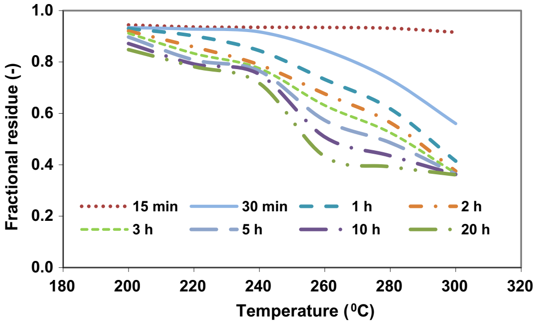

Fig. 6. Effect of temperature on fractional residue at different time instants ($D = 25.4$ mm, $L = 152.4$ mm).

particular size ($D = 25.4$ mm, $L = 152.4$ mm) in Fig. 6. It is evident that for all particle sizes, as the residence time increases the fractional residue decreases. The process is very slow till 240 °C even after 20 h of residence time and the volatile yield is very low leaving behind 72% residual char. However, in the temperature range of 260–280 °C the residual mass reduces drastically to 40%. At 290 °C a residence time of 10 h produces 40% residual char and may be considered to be optimum temperature and residence time in industrial torrefier for poplar wood. These values as well as the mass yield attained have important practical significance in deciding the residence time and the temperature in the torrefier.

3.3.2. Effect of particle size on torrefaction

Torrefaction characteristics of a large biomass particle are largely influenced by heat transfer, which is guided by its size. This effect is investigated in detail by model simulation. The simulation is carried out at a torrefier temperature of 290 °C, which is identified as the optimum reaction temperature (Section 3.2.1). Fig. 7, presenting the fractional residue for different particle diameters of length 152.5 mm each at different residence times (15 min, 30 min, 1 h, 3 h, 5 h and 10 h), reveals some interesting torrefaction behaviour. For a low residence time of 15 min, the fractional residue is hardly influenced by particle size for small particles (<16 mm) due to low heat transfer resistance. For larger particles (>16 mm) fractional residue increases with particle size for heat transfer resistance. However, after 30 min the exothermic torrefaction reaction rate is high enough to heat up the larger particles (>16 mm) much above the torrifier temperature. This causes faster reaction for larger particles leading to lower fractional residue than smaller particles. For a reactor temperature of 290 °C the average particle temperature is 314, 301 and 297 °C for 24 mm, 16 mm and 4 mm diameter particles respectively. This makes large hotter particles react faster than the small colder paricles. The residue becomes nearly constant above particle size of 24 mm.

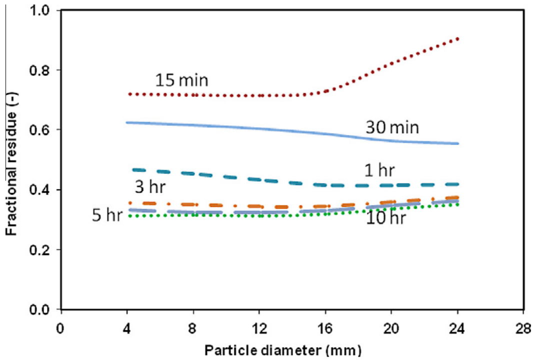

Fig. 7. Effect of residence time and particle size on fractional residue for torrefaction cylindrical wood particles at 290 °C ($D = 25.4$ mm, $L = 152.4$ mm).

After a residence time of 3 h the primary reaction is almost complete and the torrefaction reaction proceeds through secondary reaction only by slow decomposition of C^*. The above heating up effect gradually disappears and the normal trend of increase of fractional residue with particle size due to larger heat transfer resistance is observed at higher residence times.

4. Conclusions

Simple parallel kinetic schemes are proposed for both primary and secondary reactions for torrefaction of large wet wood particles. Drying and heat transfer is also incorporated to investigate the torrefaction behaviour . The predicted results show good agreement with the experimental results. The simulation results show that the average particle temperature lies about 10–15 °C above the reactor temperature which favours the torrefaction. The optimum torrefaction temperature, particle size and residence time are assessed through model simulation and estimated to be 290 °C, 24 mm and 10 h respectively under the given conditions.

References

Arias, B., Pevida, C., Fermoso, J., Plaza, M.G., Rubiera, F., Pis, J.J., 2008. Influence of torrefaction on the grindability and reactivity of woody biomass. Fuel Process. Technol. 89, 169–175.

Bates, R.B., Ghoniem, A.F., 2013. Biomass torrefaction: Modeling of reaction thermochemistry. Bioresour. Technol. 134, 331–340.

Boroson, M.L., Howard, J.B., Longwell, J.P., Peters, A.W., 1989. Product yield and kinetics from the vapor phase cracking of wood pyrolysis tars. AIChE J. 35, 120–128.

Bradbury, A.G.W., Sakai, Y., Shafizadeh, F., 1979. A kinetic model for pyrolysis of cellulose. J. Appl. Polymer Sci. 23, 3271–3280.

Bryden, K.M., Hagge, M.J., 2003. Modeling the combined impact of moisture and char on the pyrolysis of a biomass particle. Fuel 82, 1633–1644.

Chen, W.H., Kuo, P.C., 2011. Torrefaction and co-torrefaction characterization of hemicellulose, cellulose and lignin as well as torrefaction of some basic constituents in biomass. Energy 36, 803–811.

Chen, W.H., Lu, K.M., Lu, S.H., Tsai, C.M., Lee, W.J., Lin, T.C., 2013. Biomass torrefaction characteristics in inert and oxidative atmospheres at various superficial velocities. Bioresour. Technol. 146, 152–160.

Chen, W.H., Wu, W.Y., Chang, J.S., 2014. Isothermal and non-isothermal torrefaction character-istics and kinetics of microalga *Scenedesmus obliquus* CNW-N. Bioresour. Technol. 155, 245–251.

Ciolkosz, D., Wallace, R., 2011. A review of torrefaction for bioenergy feedstock production. Biofuels Bioprod. Biorefin. 5 (3), 317–329.

Di Blasi, C., 1996. Heat momentum and mass transport through a shrinking biomass particle exposed to thermal radiation. Chem. Eng. Sci. 51, 1121–1132.

Di Blasi, C., 2008. Modeling of chemical and physical processes of wood and biomass pyrolysis. Prog. Energy Combust. Sci. 34, 47–90.

Di Blasi, C., Lanzetta, M., 1997. Intrinsic kinetics of isothermal xylan degradation in inert atmosphere. Appl. Pyrolysis 40–41, 287–303.

Gaur, S., Reed, T.B., 1998. Thermal Data for Natural and Synthetic Materials. Marcel Dekker, New York.

Huang, Y.F., Chen, W.R., Chiueh, P.T., Kuan, W.H., Lo, S.L., 2012. Microwave torrefaction of rice straw and pennisetum. Bioresour. Technol. 123, 1–7.

Kersten, S.R.A., Wang, X., Prins, W., Van Swaaij, W.P.M., 2005. Biomass pyrolysis in a fluidized bed reactor. Part 1: Literature review and model simulations. Ind. Eng. Chem. Res. 44, 8773–8785.

Koufopanos, C.A., Papayannakos, N., Maschio, G., Lucchesi, A., 1991. Modeling of the pyrolysis of biomass particles. Studies on kinetics, thermal and heat transfer effects. Can. J. Chem. Eng. 69, 907–915.

Li, H., Liu, X., Legros, R., Bi, X.T., Lim, C.J., Sokhansanj, S., 2012. Torrefaction of saw dust in a fluidized bed reactor. Bioresour. Technol. 103, 453–458.

Murugan, P., Mahinpey, N., Mani, T., Freitag, N., 2009. Pyrolysis and combustion kinetics of fosterton oil using thermogravimetric analysis. Fuel 88, 1708–1713.

Prins, M.J., Ptasinski, K.J., Janssen, F.J.J.G., 2006. Torrefaction of wood Part 1. Weight loss kinetics. J. Anal. Appl. Pyrol. 77, 28–34.

Rousset, P., Turner, I., Donnot, A., Perré, P., 2006. The choice of a low-temperature pyrolysis model at the microscopic level for use in a macroscopic formulation. Ann. Sci. 63, 213–229.

Saastamoinen, J.J., Taipale, R., Horttanainen, N., Sarkomaa, P., 2000. Propagation of ignition fronts in beds of wood particles. Combust. Flame 123, 214–226.

Sadhukhan, A.K., 2010. Modelling and simulation of pyrolysis and combustion of coal and bio- mass (Ph.D. thesis). National Institute of Technology, Durgapur, India.

Sadhukhan, A.K., Gupta, P., Goyal, T., Saha, R.K., 2008. Modelling of pyrolysis of coal–biomass blends using thermogravimetric analysis. Bioresour. Technol. 99, 8022–8026.

Sadhukhan, A.K., Gupta, P., Saha, R.K., 2009. Modelling of pyrolysis of large wood particles. Bioresour. Technol. 100, 3134–3139.

Sarvaramini, A., Assima, G.P., Larachi, F., 2013. Dry torrefaction of biomass – Torrefied products and torrefaction kinetics using the distributed activation energy model. Chem. Eng. J. 229, 498–507.

Varhegyei, G., Bobaly, B., Jakab, E., Chen, H., 2011. Thermo gravimetric study of biomass pyrolysis kinetics, A distributed activation energy model with prediction tests. Energy Fuels 25, 24–32.